

CRYSTALLIZATION OF ISOTACTIC POLY(PROPYLENE) IN SOLUTION AS FOLLOWED BY SLOW CALORIMETRY

Hong PHUONG-NGUYEN and Genevieve DELMAS*

*Département de chimie,**Université du Québec à Montréal, C.P.8888, Succ. Centre-Ville, Montréal, Québec, H3C 3P8 Canada*

Received May 29, 1995

Accepted July 11, 1995

Dedicated to Dr Blahoslav Sedlacek on the occasion of his 70th birthday.

Dissolution, crystallization and second dissolution traces of isotactic poly(propylene) have been obtained in a slow temperature ramp (3 K h^{-1}) with the C80 Setaram calorimeter. Traces of phase-change, in presence of solvent, are comparable to traces without solvent. The change of enthalpy on heating or cooling, ΔH_{total} , over the 40–170 °C temperature range, is the sum of two contributions, ΔH_{DSC} and $\Delta H_{\text{network}}$. The change ΔH_{DSC} is the usual heat obtained in a fast temperature ramp and $\Delta H_{\text{network}}$ is associated with a physical network whose disordering is slow and subject to superheating due to strain. When dissolution is complete, ΔH_{total} is equal to ΔH_0 , the heat of fusion of perfect crystals. The values of ΔH_{total} for nascent and recrystallized samples are compared. Dissolution is the tool to evaluate the quality of the crystals. The repartition of ΔH_{total} into the two endotherms, reflects the quality of crystals. The crystals grown more rapidly have a higher fraction of network crystals which are stable at high T in the solvents. A complete dissolution, i.e. a high temperature (170 °C or more) is necessary to obtain good crystals. The effect of concentration, polymer molecular weight and solvent quality on crystal growth is analyzed.

The physical and thermal properties of slowly crystallized isotactic poly(propylene) (iPP) have been investigated over the last 30 years by several laboratories^{1–10}. The melting properties of perfect crystals i.e. their melting temperature, T_0 , and their heat of fusion ΔH_0 , have been established^{1,2}. A calorimetric crystallinity, α_c , of semi-crystalline samples is obtained using accepted values of ΔH_0 . The value of α_c , for a highly stereoregular sample, does not exceed 0.55. However, the crystalline fraction measured either by X-ray diffraction^{2,11,12} or by density^{3,8,12,13} is about 0.74 for most samples. Other techniques to measure the mobility such as the spin relaxation of the proton^{14–16} also find a high fraction (0.8) of rigid chains.

* The author to whom correspondence should be addressed.

The calorimetric determination of crystallinity rests on the amount of meltable fraction and in the usual practice of DSC on the amount of order meltable in a short time (typically less than 10 min). Since the measurable enthalpy of melting was not found to depend on the rate of heating, over a range of temperature compatible with the DSC apparatus (about 2–20 K min⁻¹), it was concluded that all meltable order was destroyed in the usual conditions of the DSC measurements. There were however, frequent reports suggesting an incomplete melting of the crystals by the DSC techniques¹⁷. Recent investigations show that the missing enthalpy is indeed detectable but only with calorimeters whose range of stability and sensitivity do not overlap with those of the DSC apparatus. The discrepancy between the calorimetry analysis and the others can be reduced by using the new technique of slow calorimetry^{13,18–21,23–26} described briefly below.

Slow Calorimetry of Semi-Crystalline Polyolefins: Evidence of a Semi-Ordered Physical Network

The model of a semi-crystalline polymer developed from the results of slow calorimetry appears to bring new information on ill-understood effects such as specific properties of nascent polymers, gel formation¹⁸, superheating¹⁹, maximum drawability¹⁹ and chain dynamics at the first melting²² and in solution^{23,24}. The main features of the results obtained for poly(ethylene) (PE)^{17–24} and iPP^{13,25} which appear to form a general pattern for chain molecules will be recalled below.

Two kinetics of melting are found in a typical trace. The total enthalpy, ΔH_{total} , is written as the sum of two contributions:

$$\Delta H_{\text{total}} = \Delta H_{\text{DSC}} + \Delta H_{\text{network}} \quad (1)$$

The endotherm with a fast kinetics, ΔH_{DSC} , is the heat of fusion measured by fast calorimetry i.e. the heat of fusion of the main crystals which are the orthorhombic crystals for PE and the monoclinic crystals for iPP. The crystallinity calculated from ΔH_{DSC} comes from the long-range order measured by WAXR diffraction. The endotherm with a slow kinetics, $\Delta H_{\text{network}}$, has been associated with the enthalpy of disordering a physical network which is endowed with short-range order. The second contribution of Eq. (1) which is sizeable, raises the enthalpy of fusion by half or a third. It raises also the calorimetric crystallinity.

An intriguing feature of ΔH_{total} is that for linear PE and highly isotactic poly(propylene), it is equal to ΔH_0 within the limits of the measurements. This result suggests a reconsideration of the meaning of the cohesive energy and of the meltable energy in semi-crystalline polymers.

The phase change with slow kinetics is reversible. For PE and iPP crystallized from the melt, the endotherms with slow kinetics seen on the heating trace appear as exotherms on the crystallization trace. Schematic crystallization traces (heat flow, Φ) are similar to Fig. 1 with the temperatures displaced.

Strain Melting and Strain Dissolution

The schematic Fig. 1 shows the main peak, the flat endotherms and a region of arrested melting. The parameters of the main peak (T_m and ΔH_m) are usually identical in the DSC or slow melting measurements. The endotherm with a slow kinetics occurs partly below and partly above T_m with some overlapping with the main peak. Melting temperatures below T_m may be explained by the small size or imperfections of the crystals. However, high values of T_m , particularly those above T_0 , require a different explanation. The latter resides in the building up of strain between the chains in the temperature ramp (T-ramp). This has the effect of raising T_m , a well-known phenomena described as superheating¹. The building up of strain has another more radical effect on the network crystals. It makes them unmeltable^{1,17} in the conditions of the DSC and often not completely melted in the slow calorimetry^{18,19}.

The temperature of phase-change of the network phase and $\Delta H_{\text{network}}$ itself are highly dependent on heating rate and on previous treatment. The differences reflect different phase composition in the sample which have been correlated with a range of maximum drawability for PE films²⁰. The melting characteristics of crystals with the long-range order, on the other hand, are relatively insensitive to the sample history.

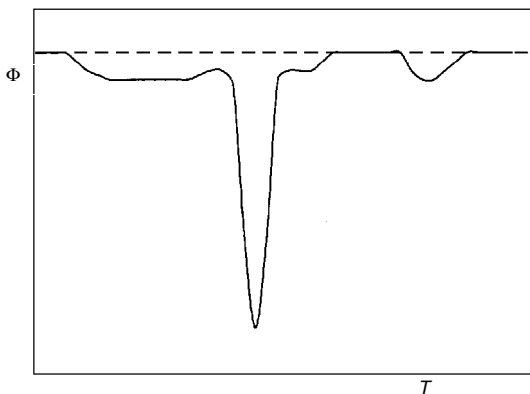


FIG. 1

Schematic representation of the melting trace (heat flow, Φ) of a semi-crystalline polyolefin in a slow T-ramp. The new result is the endotherm with a slow kinetics. It is associated with the disordering of a physical network. A region of arrested melting is seen below the high-temperature endotherm

The effect of strain on the phase-change of the network has been presented for PE (refs¹⁷⁻²⁴) and iPP (refs^{13,25}). A model for the irreversible change at the first melting of a nascent sample has been proposed²¹. During the T-ramp, a temperature-dependent expansion occurs which becomes more dramatic at the melting temperature due to the change of volume of melting, V_m . Due to the interconnection of free chains and network chains, the effect of V_m on the network is unescapable, the loose network of the nascent polymer becomes at melting, a tight network²¹. Furthermore, part of the ordered chains in the network become more strained as T increases. The high-temperature endotherm in Fig. 1 corresponds to the melting of the strained chains of the network. The non-reversible character of the slow melting endotherm comes from the density of entanglements in the physical network and the building up of strain which are both kinetically controlled.

In the experiments using slow melting, accurate measurements of ΔH_{total} give an important information. A high value of ΔH_{total} means that the melting is complete. The temperature reached in the trace has been sufficient to overcome the actual strain in the crystals and melt them. A low value indicates that unmelt crystals stay in the melt or in the solution because the kinetics of strain building has been dominant. Strategies which can reduce the strain on melting are desirable as explained below.

Strategies to Reduce the Strain

If strain could be reduced during the expansion, the range of temperature needed to melt the network will be reduced, melting will be more complete and ΔH_{total} more precise. The efficiency of the strategy can be followed on a given sample by the value of ΔH_{total} obtained in the whole temperature-range of the measurement. A strategy has been applied for nascent iPP in the literature. It consists in melting the nascent crystals at high temperature well above T_m and recrystallizing slowly. ΔH_{total} of the recrystallized sample is larger than ΔH_{total} of the nascent. In the case of iPP, one should mention that the nascent and the recrystallized samples have a different X-ray diagram.

For PE, iPP, and poly(4-methylpentene) (P4MP), another strategy was used^{13,25-27}. Melting is achieved on a solid substrate such as glass beads or metallic powders (Cu, stainless steel, Al). The strategy is very successful in lowering the range of temperature of the slow endotherms and in increasing ΔH_{total} . It does not change ΔH_{DSC} . The mechanism of action of melting on a solid is not quite clear but seems to be associated with a microphase-separation between the molecules of different mobility. Separation is known to take place on crystallization but it exists also on melting²⁸. Since a solid surface favors the recrystallization during melting in the low-temperature part of the endotherm, it will enhance phase separation. Due to their difference in mobility²⁹, the network and the free molecules should have a different rate of adsorption at the solid-melt interface. Once separated, the expansion due to the temperature ramp and to the volume of melting causes less strain.

Heats of Dissolution

In the present paper, the heats of dissolution of iPP samples are presented. The solvent will be used to induce the microphase separation i.e. to make ΔH_{total} complete. The role of a solvent in chain dynamics has been observed²⁴ on the heats of dissolution of high molecular weight PE. It was found that when a nascent sample is dissolved in different solvents, the fraction of the chains which are caught in the network is solvent-dependent. In volatile solvents, ΔH_{DSC} is found lower because a larger proportion of the chains is caught in the network phase at the dissolution. It will be shown below that only high dilutions lead to a complete dissolution with $\Delta H_{\text{total}} = \Delta H_0$.

The thermodynamics of poly(propylene) solutions has focussed on certain points such as the effect of the difference in free volume between polymer and solvent^{15,16,30} or the characterization at a lower critical solution temperature (LCST) (ref.³¹). The swelling of iPP samples in solvents and the formation of thermoreversible gels have also been investigated^{33,34}. Heats of dissolution have been scarce due to the lack of an adequate apparatus.

EXPERIMENTAL

Materials

Highly stereoregular nascent samples of isotactic poly(propylene) (iPP) were made by Himont at Varennes, Québec, Canada (sample F) or at Wilmington, Delaware, U.S.A. (sample U). Their characteristics are given in Table I. The different X-ray diagrams of nascent and recrystallized iPP have been interpreted recently³⁵. Solvents are from Aldrich Chemicals (99% purity).

Thermal Stability of iPP

The stability of iPP solution has been investigated in the course of the fractionation and molecular weight distribution determination at a LCST (ref.³¹). Polymer and solvent are placed in a glass tube which is sealed after being thoroughly flushed by nitrogen. Degradation can be avoided, even at high temperature, if an antioxidant, such as Irganox, is added to the solvent.

Calorimetric Procedure

The sensitive C80 Setaram calorimeter is used as in previous work¹⁷⁻²⁴ with a 3 K h⁻¹ T-ramp. The glass tube containing polymer, solvent and antioxidant is equilibrated during 17 h at the same temperature as the T-ramp is started (20 °C). Stirring is effected by rotating the calorimeter through 180°.

Three or more traces can be obtained on the same solution. The first dissolution, first crystallization, and second dissolution are reported in the present work. The thermal history of each solution such as quenching, slow crystallization, aging is recorded.

Crystals. The dissolution traces are presented for two types of crystals. The nascent crystals of the as-received powder and the crystals grown in solution.

Crystal growth. In the present procedure, there are four differences from the usual crystallization in solution. They concern the concentration, the temperature during crystallization, the residence in the mother-solution and the maximum temperature of the solutions, T_{max} : (i) For the dilute solution

TABLE I
Characteristics of iPP samples as received and after high temperature treatment

Sample	Characterization ^a		Fast DSC ^b		d g cm ⁻³	Crystallinity as received		Crystallinity after melting/crystallization ^c			
	$10^{-3}M_w$	M_w/M_n	T_m , °C	H_m , J g ⁻¹		$\alpha_c(d)$	$\alpha_c(X\text{-ray})^c$	$\alpha_c(\Delta H)^d$	$\alpha_c(d)$	$\alpha_c(X\text{-ray})^c$	$\alpha_c(\Delta H)^d$
F	300	3	163	87	0.8994	0.55	0.50	0.42	0.71	0.74	0.80
U	1 000	-	165	91	0.8996	0.55	0.52	0.44	0.72	0.75	0.78

^a By turbidity at the LCST (ref.³²), ^b $v = 10$ K min⁻¹, ^c The X-ray pattern of nascent and recrystallized iPP are different³⁵, ^d Using ΔH_0 208 J g⁻¹ and $\Delta H_{\text{exp}} = \Delta H_{\text{DSC}} + 0.5 \Delta H_{\text{network}}$. See refs.^{13,25} for details.

range whose results are given here, the concentrations of the solutions are spread from 0.2 to 1.3%. The high value (1.3%) is not usually considered suitable for preparing single crystals. (ii) The crystals are grown in a T-ramp rather than isothermally. For most of the experiments where crystallization is recorded, the T-ramp is 3 K h^{-1} and for the one made outside the calorimeter it is 0.2 K h^{-1} . (iii) The crystals are not dried for analysis. The parameters of the crystallization trace and those of the dissolution trace constitute the mode of analysis of these crystals. (iv) The solutions stay a long time at high temperature before they crystallize. For instance, from the end of the main dissolution peak up to T_{max} and down to T_{c} , the total time is more than two days. It is exactly 60 h for $T_{\text{d}} = 120 \text{ }^{\circ}\text{C}$, $T_{\text{max}} = 180 \text{ }^{\circ}\text{C}$, $T_{\text{c}} = 60 \text{ }^{\circ}\text{C}$, and a rate $v = 3 \text{ K h}^{-1}$. (T_{d} and T_{c} are the temperatures of the maximum of the peak of dissolution and of crystallization, respectively, in the given temperature ramp.) During that time, the heat flow corresponding to the slow disordering or ordering of the network is recorded.

Dissolution and crystallization traces. The base line has been subtracted to eliminate the awkward slanted profile presented in previous publications. The base line is constructed for each experiment by using the points between the beginning of the dissolution and other points, either on a region of arrested dissolution or at the end of the dissolution. Using Eq. (1), the heat of dissolution can be written as

$$\Delta H_{\text{dissolution}} = \Delta H_{\text{melting}} + \Delta H_{\text{mixing}} ,$$

$$\Delta H_{\text{dissolution}} = \Delta H + Kd_{\text{p}}(1 + \phi_{\text{p}})^{-1} = \Delta H_{\text{DSC}} + \Delta H_{\text{network}} + Kd_{\text{p}}(1 + \phi_{\text{p}})^{-1} , \quad (2)$$

where d_{p} is the density of the polymer, ϕ_{p} the volume fraction of the final solution and K is a calorimetric constant which depends on the solvent. The value of K equal to the heat of mixing, at infinite dilution, of the melt with the solvent can be estimated from the heat of mixing of a model molecule for iPP (highly branched alkane). In non-polar solvents, the third term of Eq. (2) is much smaller than those coming from $\Delta H_{\text{melting}}$ so the effect of ΔH_{mixing} will be neglected. Consequently, the heat of dissolution in J/g of polymer is identified with the heat of fusion:

$$\Delta H_{\text{dissolution}} = \Delta H_{\text{DSC}} + \Delta H_{\text{network}} . \quad (3)$$

If a range of values of $\Delta H_{\text{dissolution}}$ is found experimentally for different solvents in a DSC apparatus where $\Delta H_{\text{network}}$ is not observable, it is likely to reflect solvent-related amount of not disordered network in the solution. The result holds for other polyolefins such as PE (ref.²³) and P4MP (ref.²⁶).

Heats of dissolution have been measured as a function of ϕ_{p} up to $\phi_{\text{p}} = 0.5$ (ref.²⁷). As for PE, the fraction of $\Delta H_{\text{network}}$ meltable in the conditions of the dissolution is found to diminish rapidly with ϕ_{p} . Since the results depend on a number of factors (solvent, thermal history, molecular weight of the sample), for the sake of clarity, the data presented here will be limited to those obtained at high dilution.

RESULTS AND DISCUSSION

Enthalpy of Melting of Perfect Crystals

Single crystals of PE have been grown in solution with the objective of controlling the lamellar thickness of the lamellae, l . After drying, the characteristics of the fusion, T_m and ΔH_m , are measured as a function of l . By extrapolation to infinite thickness, the values of ΔH_0 and T_0 for a perfect crystal are obtained^{1,2}.

For iPP, the crystals grown in solution are reported not to be good crystals³⁶ and T_c does not vary with l , so the procedure used for PE is not applied to iPP. Instead, values of ΔH_0 and T_0 are obtained indirectly using melt-grown crystals. Different values for ΔH_0 and T_0 have been reported in the literature. This is due to two effects namely the limitation in the growth of well-formed crystals at high crystallization temperature and the reorganization during melting¹². The accepted values are $\Delta H_0 = 210 \text{ J g}^{-1}$ and $T_0 = 187 \text{ }^\circ\text{C}$ (ref.²). In spite of its shortcomings, crystallization in solution has been used³ to obtain iPP crystals with a high crystallinity (measured by density). In the present work, it was found that the crystals obtained from solution have crystallinity comparable to those obtained from the melt if some crystallization conditions, described below, are respected.

The findings of slow calorimetry on iPP are the following^{13,25}: ΔH_{total} is found complete (i.e. $\Delta H_{\text{total}} = 210 \pm 10 \text{ J g}^{-1}$) on recrystallized iPP and also on nascent iPP but only when melting is made on a finely divided substrate. It is incomplete on nascent iPP when the polymer melts on itself.

In this work, we would like to know the conditions required to have a complete dissolution in nascent and recrystallized iPP, to evaluate T_d values as tracers of strain melting/dissolution and also obtain direct information from the crystallization traces on conditions of crystal growth in solution.

Dissolution Traces of Solution-Grown Crystals

Nascent iPP crystals have been dissolved, slowly recrystallized and redissolved. The presentation will not follow the chronological order but rather the inverse order. Since recrystallized rather than nascent polymer has been more the focus of interest than nascent polymer, the dissolution trace of recrystallized crystals will be presented first then followed by the crystallization trace and in the third part the dissolution of the nascent samples. However, the characteristics of the phase-changes in a given solution can be followed in the corresponding rows of Tables II–IV by reading the values of T_d , T_c , ΔH_{total} , ΔH_{DSC} , $\Delta H_{\text{network}}$ which correspond to the same value of m_p (mg). The relative value of ΔH_{DSC} and $\Delta H_{\text{network}}$ changes from $n = 1$ to $n = 3$. Small differences may be due to the decomposition but larger ones have a physical meaning. Tables II–IV

give the characteristics of the redissolution, crystallization and dissolution traces in a slow T-ramp.

The first columns of Table II give the sample name (F or U), the solvent (*p*-xylene, cumene, and dodecane), the weight of polymer, the temperature of the main peak, and

TABLE II
Dissolution traces of iPP samples after a slow crystallization in solution at 3 K h^{-1} (the heating rate of 3 K h^{-1})

Sample	Solvent (4 cm^3)	m_p mg	T_d $^{\circ}\text{C}$	ΔH_{total} J g^{-1}	ΔH_{DSC} J g^{-1}	$\Delta H_{\text{network}}^a, \text{J g}^{-1}$		T_{max} $^{\circ}\text{C}$	Figure
						low T	high T		
F^b	<i>p</i> -xylene	9.80	111.1	212 (C)	176 (93–118)	26 (69–92)	10 (118–127)	135	2a
F	<i>p</i> -xylene	9.56	111.0	169 (I)	90 (96–115)	–37 (26–54)	–71 (115–136)	180	2b
						37 (54–96)	150 (136–175)		
U	<i>p</i> -xylene	9.43	116.2	211 (C)	110 (97–124)	–10 (36–68)	101 (124–155)	170	
						10 (68–91)			
F	cumene	9.91	115.6	205 (C)	145 (97–121)	–95 (32–73)	–55 (123–139)	170	
						60 (75–97)	150 (141–165)		
U	cumene	10.95	120	225 (C)	105 (109–124)	–60 (30–71)	–20 (124–135)		
						65 (75–109)	135 (135–169)		
U	cumene	49.08	117.3	214 (C)	138 (100–124)	46 (50–100)	–5 (124–132)	170	
							35 (132–161)		
F	dodecane	9.94	130.0	197 (C)	77 (120–139)	78 (41–88)	100 (139–170)	185	
						–58 (88–120)			
F	dodecane	35.52	129.2	180 (I)	140 (87–138)	20 (27–68)	20 (138–173)	200	
U	dodecane	35.51	134.0	222 (C)	120 (122–141)	35 (65–117)	67 (141–171)	200	

^a The negative values correspond to a recrystallization. ^b This sample was crystallized at 0.2 K h^{-1} .

ΔH_{total} with (C) for complete or (I) for incomplete values. As seen in Table I, U and F are abbreviations for an ultrahigh molecular weight and a high molecular weight sample. In the next columns, the details of the two contributions to ΔH_{total} , ΔH_{DSC} , and $\Delta H_{\text{network}}$ are given and the temperature intervals over which the integration has been made. The negative sign of $\Delta H_{\text{network}}$ in the dissolution traces indicates a recrystallization.

Typical dissolution trace with two kinetics of dissolution (Fig. 2a) corresponds to the first row in Table II. The value of ΔH_{total} is 212 J g^{-1} so it is marked as complete. This is the only dissolution trace of crystals grown in the very slow T-ramp (0.2 K h^{-1}). Only a fraction equal to 10 J g^{-1} of the endotherm with a slow kinetics is situated above the main endotherm. The value of ΔH_{DSC} has been calculated by integration of the heat flow between 93 and $118 \text{ }^\circ\text{C}$. Similar intervals are used on other traces where sometimes the division is not so clear as in Fig. 2a. The trace of the dissolution of the slowly crystallized crystals compares well with the melting of the same crystals¹³ with a displacement towards the low temperature range of about 60 K (i.e. $170 \text{ }^\circ\text{C}$ (T_m) – $111 \text{ }^\circ\text{C}$ (T_d)). The value of T_d , the maximum of the dissolution of the monoclinic crystals reflects the quality of the solvent and mainly its size in non-polar systems. It is $111\text{--}120 \text{ }^\circ\text{C}$ for *p*-xylene and cumene and $129\text{--}134 \text{ }^\circ\text{C}$ for dodecane. The values of Table II show that dissolution is complete for all the concentrations and is not dependent on the solvent.

The repartition of ΔH_{DSC} and $\Delta H_{\text{network}}$ varies with the conditions of crystallization. The difference between the traces of Fig. 2a and Fig. 2b illustrates the large increase in stability brought about by the very slow crystallization. In Fig. 2b ($m = 9.56 \text{ mg}$), the crystals were grown at $v = 3 \text{ K h}^{-1}$ instead of $v = 0.2 \text{ K h}^{-1}$. One sees that dissolution leads also to a value of ΔH_{total} which is incomplete. However, the repartition of the

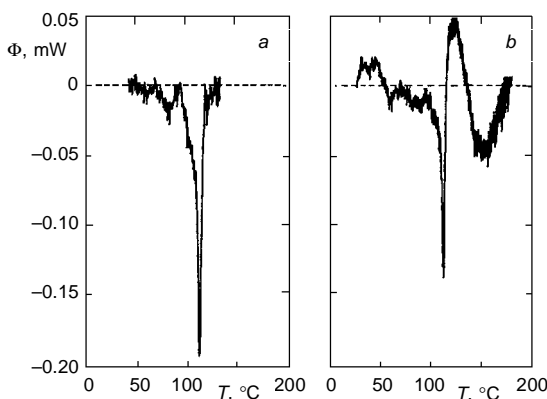


FIG. 2

Effect of the crystallization conditions on the dissolution trace at 3 K h^{-1} . Sample F crystallized in *p*-xylene in very different T-ramps (K h^{-1}): a 0.2 (data in row 1 of Table II), b 3 (data in row 2 of Table II)

enthalpies is different for the crystals grown at different rates. The unique features of the crystals crystallized more rapidly (3 K h^{-1}) namely the recrystallization above T_d and the large value of $\Delta H_{\text{network}}$ (between 115 and $175 \text{ }^\circ\text{C}$) do not depend on the perfect exactitude of the decomposition.

The traces of Figs 2a, 2b and those in the same conditions permit to arrive to two conclusions concerning the crystals grown at $\nu = 3 \text{ K h}^{-1}$. The expected conclusion is

TABLE III
Crystallization traces of iPP samples in solution at a cooling rate of 3 K h^{-1}

Sample	Solvent (4 cm^3)	m_p^a mg	T_d $^\circ\text{C}$	ΔH_{total} J g^{-1}	ΔH_{DSC} J g^{-1}	$\Delta H_{\text{network}}, \text{J g}^{-1}$		T_{max} $^\circ\text{C}$	Figure
						low T	high T		
F	<i>p</i> -xylene	9.9					45 (93–69)	150	
F	<i>p</i> -xylene	9.56	60.7	175 (I)	40 (66–49)	55 (45–22)	5 (157–143) 75 (136–66)	170	3a
U	<i>p</i> -xylene	9.43	60.0	197 (C)	160 (66–50)	27 (50–40)	$10^{a,b}$ (74–66)	170	
F	cumene	9.91	57.0	222 (C)	135 (64–48)	0	87^a (72–64)	170	
U	cumene	10.95	62.2	202 (C)	152 (71–53)	50 (53–50)	$0^{a,b}$	170	
U	cumene	49.08	59.5	230 (C)	155 (72–48)	20 (48–30)	55 (111–72)	170	3b
F	dodecane	9.94	63.0	200 (C)	70 (83–46)	0	110 (153–105) 20 (105–83)	170	
F	dodecane	35.52	69.4	~ 110 (I)	~ 75 (81–50)	0	10 (153–135) 25 (135–98)	170	
U	dodecane	35.51	77.5	210 (C)	150 (86–49)	0	60 (130–86)	170	

^a The dissolution of network was observed on cooling at high temperature. ^b Note that the beginning of the high-temperature endotherm varies widely with the sample.

that their monoclinic content is lower than for the slowly grown crystals and the unexpected conclusion is that their non-monoclinic content has a higher overall temperature stability (50 K above T_d). It is possible that the crystals with short-range order interact more with the solvent and are more susceptible to strain and deformation leading to their temperature stability. An association with another situation comes to mind: gels are formed from easily crystallizable ultrahigh molecular weight poly(ethylene) (UHMWPE) by quenching solutions whose concentration is of a few percent. Although cooling at 3 K h⁻¹ between 170 °C and room temperature, is hardly comparable to a quenching procedure, the similarity in the two systems of leaving less time for the crystals to grow should not be overlooked. This result could offer a guiding strategy to prepare, in more concentrated solutions, iPP gels, highly stable in temperature.

Information Given by the Crystallization Traces on Modes of Crystal Growth in Solution

The organization of Table III is similar to that of Table II with T_c replacing T_d . Crystallization is complete except for two traces which will be commented below. However, the distribution of ΔH_{total} between ΔH_{DSC} and $\Delta H_{\text{network}}$ varies widely from one row to another. The following examples illustrate the effect of three parameters, on the distribution, of ΔH_{total} between ΔH_{DSC} and $\Delta H_{\text{network}}$. These are the solution concentration, the polymer molecular weight and the value of T_{max} , the maximum temperature of residence of the solution before the initiation of the T-ramp. The concentration will not be characterized in g/cm³ but only in mg since as said in the experimental part, the volume of solvent is always the same in the dilute solution.

The crystallization of sample F in *p*-xylene with $m_p = 9.56$ mg (0.24%) is shown in Fig. 3a, that of sample U in cumene with $m_p = 49.08$ mg (1.3%) is given in Fig. 3b. In the dilute solution, $\Delta H_{\text{network}}$ (135 J g⁻¹) is spread between 157 and 22 °C while the main crystals grow in a smaller quantity ($\Delta H_{\text{DSC}} = 40$ J g⁻¹) between 66 and 49 °C with a peak at 60.7 °C. In the more concentrated solution, $\Delta H_{\text{network}}$ (75 J g⁻¹) is spread between 111 and 30 °C while the main crystals grow in an larger quantity ($\Delta H_{\text{DSC}} = 155$ J g⁻¹) over the same temperature range as in the dilute solution. The balance between $\Delta H_{\text{network}}$ and ΔH_{DSC} is inverted in the two solutions. The fraction of monoclinic crystals compared to the network crystals, grown in the 3 K h⁻¹ temperature ramp is low if they grow in very dilute solution but larger if grown in the 1.3% solution.

Interestingly, the dissolution traces confirm the crystallization traces since ΔH_{DSC} for sample F is lower than for sample U as in the crystallization trace. However, the dissolution traces give another piece of information. Maturation or aging has taken place for the monoclinic crystals suspended in the dilute solution since, for sample F, ΔH_{DSC} has increased from a low value of 40 J g⁻¹ in the crystallization trace to a value of about 90 J g⁻¹ in the dissolution trace. On the other hand, ΔH_{DSC} has not changed much from the

crystallization trace (155 J g^{-1}) to the dissolution trace for the more concentrated solution.

Effect of Molecular Weight

The effect of the sample molecular weight, in the crystallization, can be seen by comparing the last two rows. The solutions have the same concentration (with 35.52 and 35.51 mg) but the M_w of U (last row) is higher than that of F. The difference between the modes of crystallization can be seen on the data of Table III. The temperature of the main crystallization peak is higher ($77.5 \text{ }^\circ\text{C}$) for U than for F ($69.4 \text{ }^\circ\text{C}$). The trace similar to that of Fig. 3b does not indicate a separation between the peaks for ΔH_{DSC} and $\Delta H_{\text{network}}$. The peaks are distinguishable but they overlap. The crystallization trace of sample F on the other hand shows two separated exotherms. Sample F has a lower value of ΔH_{total} and the main peak is wide and incomplete with ΔH_{DSC} about 75 J g^{-1} . The slower crystallization rate of sample F does not have irreversible consequences as indicated by the recovery of the crystals. The dissolution trace of the same crystals F shows an almost complete ΔH_{total} (180 J g^{-1}) with $\Delta H_{\text{DSC}} = 140$ and $\Delta H_{\text{network}} = 40 \text{ J g}^{-1}$ as listed in Table II. This constituted another case of crystal maturation in solution.

Effect of T_{max}

The first line of Table III ($m = 9.9 \text{ mg}$) gives the case of a solution cooled after a low T_{max} ($150 \text{ }^\circ\text{C}$ instead of the usual $170 \text{ }^\circ\text{C}$). The crystallization is highly incomplete with a flat exotherm. If these crystals were separated from the solution at the end of the

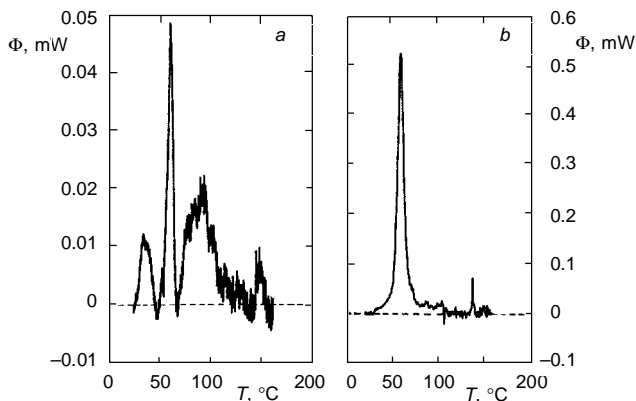


FIG. 3

Crystallization traces, at 3 K h^{-1} , in different conditions showing **a** the separation of the network and monoclinic crystals (sample F, data in row 2 of Table III) or **b** their partial co-crystallization (sample U, data in row 6 of Table III)

crystallization they would not appear perfect. A second and a third dissolution, the results of which are not listed in Table II, indicate that these crystals do not cure between crystallization and dissolution if the maximum temperature stays at 150 °C. In consequence, the crystallizations after a low value of T_{\max} were discontinued.

Effect of the Solvent on the Co-Crystallization of Monoclinic Crystals and Network Crystals

As said above, the separation of the peaks of the two endotherms depends on the sample molecular weight (see the last two rows in dodecane with $m_p = 35.5$ mg). It is also influenced by the nature of the solvent. The extent of co-crystallization can be evaluated in Table III from the temperature interval under the figures for the enthalpies. In Fig. 3a, co-crystallization does not take place extensively since the high temperature endotherm starts at 157 °C while the main peak is at 66 °C. Among the four other cases of crystallization in dilute solution three of them (in *p*-xylene and in cumene) are examples of co-crystallization since the beginning of crystallization of the network is lower than 75 °C. These are for F (9.91) and U (10.95) in cumene and U (9.43) in *p*-xylene. In Fig. 4, the trace of crystallization of sample F ($m_p = 9.91$ mg) in cumene is given. Observed rapidly, the trace could be deceiving and led to the identification of a single morphology, the bump in the peak explained by an increase of growth rate around 64 °C. With an unambiguous ΔH_{total} equal to 222 J g⁻¹, a crystal with a huge amount of long-range order (about 100%) could be expected. However, when the analysis is made in context with the other crystallization traces, one recognizes that this peaks reveals that even in dilute solution, short-range and long-range order can co-crystallize on the same temperature range in the conditions of the experiment. More experiments are needed to correlate the mode of crystallization and the characteristics of the

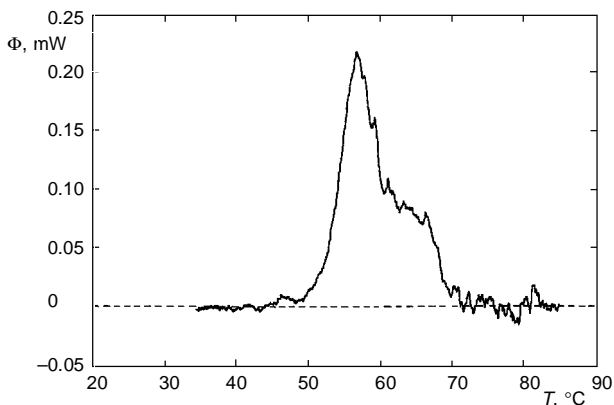


FIG. 4

Crystallization trace, at 3 K h⁻¹, of sample F. Data in row 4 of Table III showing the co-crystallization of the monoclinic and network crystals with almost the same kinetics

solvent (quality for the polymer, viscosity, free volume at T_{\max}). Non-destructive analysis of the crystals such as X-ray diffraction and density measurements will confirm the measurement of enthalpy change and their interpretation.

These results on crystallization in solution confirm, in a quantitative way the observations found in the literature concerning the sensitivity of the morphology of solution-grown crystals to the conditions of the solution. However, the importance of the high temperature of the solution has not been mentioned explicitly. The reason is the unawareness of the stability of the network crystals above T_d so that the importance of leaving the solution well above T_d was not perceived.

The maturation of crystals in a solution where ΔH_{DSC} is small and $\Delta H_{\text{network}}$ is large permit to make the hypothesis that the first step of the growth of crystals in solution is the formation of crystals with short-range order which, with time and in contact with a mobile phase will mature into the usual long-range order crystals. Since the value of ΔH_{total} does not vary much with its repartition between ΔH_{DSC} and $\Delta H_{\text{network}}$, one must conclude that the change from short-range order to long-range order is athermal. In other words, cooling a solution changes the enthalpy of the solid by about 200 J g^{-1} independent of the distribution of the organized matter between the monoclinic crystals and the network crystals.

Dissolution Traces of the Nascent Samples

The figures of Table IV for the dissolution of nascent, arranged as those in Table II for the recrystallized samples, permit the comparison between the two kinds of crystals. The two points to be noted are the following:

The dissolution of nascent iPP gives ΔH_{total} values smaller than that of the recrystallized iPP. The dissolution of the network is complete only in very dilute solutions ($m_p < 10 \text{ mg}$). As said above, ΔH_{total} is always incomplete when the nascent polymer is melted on itself but complete on a substrate. The solvent has then the same effect as the substrate in preventing the strain to build between the chains. One can understand the necessity to have a very dilute solution to achieve this aim by remembering the dependence on concentration of the Flory–Huggins equation for the chemical potential. The fast lowering of the chemical potential when the dilution increases makes the separation between molecules more rapid and drives into solution a fraction of the polymer which is otherwise unmeltable. Note that for the nascent sample only, recrystallization below T_d occurs in dilute solutions with an enthalpy which can reach -25 J g^{-1} .

The values of T_d are higher in Table IV for the nascent samples than in Table II for the recrystallized samples, a sign of strain-melting as commented upon below.

The details of the traces such as the shape of the trace, the eventual recrystallizations before or after dissolution, the variation in T_d in cases where it is not expected to vary, give some coherent information of the chain dynamics, information which may not be always clear on the tables. Traces different from the six given in this paper could have

been chosen to illustrate one interesting point or another. The traces which could not be reproduced as figures in the paper are available on request. In the paragraph below, a compelling evidence of the presence, in the clear solution, of network crystals will be given. It is related to the recrystallization at high temperature above T_d .

TABLE IV

Dissolution traces of the nascent iPP samples at a heating rate of 3 K h^{-1}

Sample	Solvent (4 cm^3)	m_p mg	T_d $^\circ\text{C}$	ΔH_{total} J g^{-1}	ΔH_{DSC} J g^{-1}	$\Delta H_{\text{network}}, \text{J g}^{-1}$		T_{max} $^\circ\text{C}$	Figure
						low T	high T		
F	<i>p</i> -xylene	9.9	115.7	219 (C)	170 (97–118)	–24 (68–79) 24 (82–97)	15 (118–127) 34 (140–156) ^a	150	
F	<i>p</i> -xylene	9.56	115.7	215 (C)	190 (72–120)	–5 (30–45) 5 (45–72)	–15 (120–134) 40 (134–145)	165	5a
U	<i>p</i> -xylene	9.43	125	190 (C)	77 (99–127)	–45 (42–69) 67 (69–98)	67 (145–172)	170	
F	cumene	9.91	115.5	199 (C)	110 (98–120)	–45 (42–69) 67 (69–98)	67 (145–172)	195	
U	cumene	10.95	129	200 (C)	110 (112–131)	–25 (51–61) 115 (69–112)	0	140	
U	cumene	49.08	128.5	149 (I)	151 (82–134)	–22 (42–82)	20 (153–179)	180	5b
F	dodecane	9.94	133.5	162 (I)	91 (121–143)	10 (55–72) 40 (86–121)	21 (148–165)	170	
F	dodecane	35.52	133	105 (I)	85 (117–138)	15 (105–117)	5 (138–150)	170	
U	dodecane	35.51	143	152 (I)	105 (123–144)	32 (96–123)	15 (152–168)	170	

^a Extrapolated value.

Recrystallization during melting has been reported for many semi-crystalline polymers. It leads to a double melting peak in fast DSC due to the melting at higher temperature of the thicker and more stable lamellae grown during recrystallization. It is rarely observed in solution (except in very low T -ramp²² (0.2 K h^{-1}) due to the slower rate of crystallization in solution.

In the network, the usual process of lamellar thickening can take place by dissolution and recrystallization of the network crystals. Recrystallizations can also occur because of the expansion during the temperature ramp. Due to it, strain increases both in the crystals and in the melt leading to an increase of T_m and recrystallization. In Fig. 5a (9.56 mg in *p*-xylene), recrystallization can be seen to occur as an exothermic effect between 120 and 134 °C, i.e. over a range of temperature 14 K higher than the end of the main peak of dissolution. Between 134 and 145 °C, dissolution resumes and possibly continues at a low rate at high temperature. The parameters regulating the chain dynamics of nascent samples are not fully understood but it seems that volatile solvents induce such a recrystallization. The solutions of UHMWPE in cyclopentane display a particularly large recrystallization peak²¹ (110 J g^{-1}). In Fig. 5b, the dissolution trace is incomplete due to the higher concentration. Other endotherms, corresponding to highly strained parts of the network would be expected to appear on the trace at temperatures higher than 180 °C. In the present solutions of iPP, or in those of PE, degradation cannot be at the origin of the exotherm.

Non-equilibrium melting/dissolution temperatures are indicative of strain. The subject has been formulated conceptually¹ but investigated mainly on PE by DSC. The

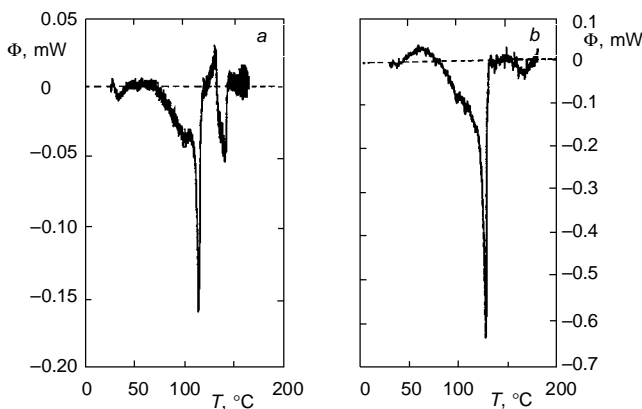


FIG. 5

Dissolution trace of nascent samples (for the dissolutions, the calorimeter is rotated): **a** sample F in dilute solution, ΔH_{total} is complete (data in row 2 of Table IV), recrystallization and melting of the network are apparent above T_d ; **b** sample U in less dilute solution, ΔH_{total} is incomplete (data in row 6 of Table IV)

second fusion of a well recrystallized sample of PE has a lower T_m , an indication of the separation of the free chains and the network chains during the first melting²¹. At the second melting, due to the separation, the strainable morphology is no longer the whole solid but only the network part. The second melting of iPP, however, does not lower T_m of the monoclinic crystals^{13,25}. This unexpected constancy in T_m has been attributed to the continual transformation of iPP crystals in the absence of solvent, a feature which masks the change of strain between T_m (nascent) and T_m (recrystallized). In presence of a solvent, on the other hand, the change in strained dissolution is clear, as seen in the change of T_d (fourth columns of Tables II and IV).

In the three solvents, the loss of the nascent character lowers T_d by about 4 K for sample F and by 9 K for sample U. Less rearrangement in presence of the solvent explains that the expected effect occurs. The effect of molecular weight is reasonable, the long chains of the high molecular weight samples lead to more strain at the first melting. It is very likely that in some solvents, more than one cycle of dissolution/crystallization is needed to diminish the strain and lead to an equilibrium value of T_d which should not depend much on the sample molecular weight. Note that in dodecane ($m_p = 35.51$) the T_d of sample U is 4 K higher than that of sample F.

Significance of the Results

The present work confirms that $\Delta H_{\text{total}} = \Delta H_0$ for the recrystallized samples at the dissolution. It shows also that the change of heat content of nascent iPP between between the solid and liquid state can be complete if the final solution is highly dilute.

The quality of the crystals grown in solution is evaluated from their dissolution trace. More precisely, it is associated with the size, ΔH_{DSC} , of the dissolution peak corresponding to the monoclinic crystals, for example, the endotherm between 93 and 118 °C in Fig. 2a. This criterium takes into account the stability of the crystals during the low T-ramp which is used for the analysis. Then, the conditions to have stable crystals can be determined. It is concluded that a high T_{max} is needed to obtain a high ΔH_{DSC} . A uniform value of 170 °C has been used in this work but lower temperatures may be sufficient in some solvents. Crystallization in a very low T-ramp from from 170 °C to room temperature lead to good crystals when they are grown in dilute solution (0.24%). A faster T-ramp and a higher concentration lead also to good crystals. Crystal maturation has been observed for crystals grown in the relatively fast T-ramp (3 K h⁻¹) but does not seem to take place when T_{max} is low.

The following view of phase change emerges from the present accurate measurement of ΔH . When a polymer solution is cooled slowly, its change of enthalpy is equal to ΔH_0 , the heat of crystallization of perfect crystals whatever the repartition of that heat between the crystals with long-range order, ΔH_{DSC} and those with short-range order, $\Delta H_{\text{network}}$. This effect is thought to be general and apply to easily crystallizable polymers.

CONCLUSION

In the past, investigation by slow calorimetry has not been made to avoid reorganization of the sample. Also, the calorimeters with the high sensitivity to measure small heat flows were not available. Moreover, the usual DSC data formed a coherent picture of semi-crystalline polymers which lead to the consensus that slow calorimetry was not necessary because all melttable order was melted in the fast T-ramp. We would like by this paper and previous ones, convince scientists interested in the field of phase-changes and chain-dynamics that this new technique is helpful in solving some long-standing problems found in the literature of polymer research. It may help to widen the definition of crystallinity of a semi-crystalline sample, throw some light on non-equilibrium melting and dissolution and give guidance to prepare stable crystals in solution, thermoreversible gels and highly drawable polymer films. The findings that the cooling of a polymeric liquid across the crystallization temperature leads to a change of enthalpy which is independent of the proportion of short- and long-range order in the crystallized solid requires a revision of accepted ideas.

While writing this paper in honor of the 70th birthday of Prof. Sedlacek, I could relive the scientific stimulation felt over the years at the occasion of the Polymer conferences organized by the Macromolecular Institute in Prague. I could relive also the fascinating immersion in the cultural life of central Europe which went with the conferences. We wish this issue of the CCCC to be a symbol of the gratitude of many scientists, including both of us, to Dr Sedlacek and his collaborators to have landmarked our careers of missions to Prague where new scientific knowledge, experiences of arts and music and expressions of friendship were so beautifully entangled.

REFERENCES

1. Wunderlich B.: *Macromolecular Physics*. Vol. 1, Academic Press, London 1973; Vol. 2, Academic Press, New York 1976; Vol. 3, Wiley, New York 1980.
2. Bu H. S., Cheng S. Z. D., Wunderlich B.: *Makromol. Chem., Rapid Commun.* 9, 75 (1988).
3. Gee D. R., Melia T. P.: *Makromol. Chem.* 132, 195 (1970).
4. Monasse B., Haudin J. M.: *Colloid. Polym. Sci.* 263, 822 (1985).
5. De Candia F., Iannelli P., Staulo O., Vittoria V.: *Colloid Polym. Sci.* 266, 608 (1988).
6. Balta Calleja F. J., Martinez Salazar J., Asano T.: *J. Mater. Sci., Lett.* 7, 165 (1988).
7. Janimak J. J., Cheng S. Z. D., Zhang A., Hsieh E. T.: *Polymer* 33, 728 (1992).
8. Samuels R. J.: *J. Polym. Sci., Polym. Phys. Ed.* 13, 1417 (1975).
9. Grebowicz J., Lau S.-F., Wunderlich B.: *J. Polym. Sci., Polym. Symp.* 71, 19 (1984).
10. Varga J., Schulek-Tot F., Ille A.: *Colloid Polym. Sci.* 269, 655 (1991).
11. Suraf R. F., Porter R. S.: *Polym. Eng. Sci.* 28, 842 (1988).
12. Mexghani K., Campbell R. A., Philips P. J.: *Macromolecules* 27, 997 (1994).
13. Xhang X., Lapes I., Phuong-Nguyen H., Delmas G.: Unpublished results.
14. Kitamaru R., Horri F., Murayama K.: *Macromolecules* 19, 636 (1986).
15. Tanaka H., Yoshida Y.: *Angew. Makromol. Chem.* 113, 31 (1983).
16. Tanaka H., Korogi F.: *Eur. Polym. J.* 24, 759 (1988).
17. Keller A., Willmouth F. M.: *J. Macromol. Sci., Phys. B* 6, 493 (1972).

18. Phuong-Nguyen H., Delmas G.: *Macromolecules* 25, 414 (1992).
19. Phuong-Nguyen H., Delmas G.: *Macromolecules* 25, 408 (1992).
20. Phuong-Nguyen H., Delmas G.: *J. Mater. Sci.* 29, 3612 (1994).
21. Delmas G.: *J. Polym. Sci., Polym. Phys. Ed.* 31, 2011 (1993).
22. Morin F., Delmas G., Gilson D.: *Macromolecules* 28, 3248 (1995).
23. Phuong-Nguyen H., Delmas G.: *Thermochim. Acta* 238, 257 (1994).
24. Phuong-Nguyen H., Delmas G.: *J. Solution Chem.* 23, 249 (1994).
25. Xhang X., Lapes I., Phuong-Nguyen H., Delmas G.: *J. Polym. Sci., Polym. Phys. Ed.*, in press.
26. Phuong-Nguyen H., Delmas G.: *J. Therm. Anal.*, in press.
27. Phuong-Nguyen H., Delmas G.: Unpublished results.
28. Wunderlich B.: *Faraday Discuss., Chem. Soc.* 68, 239 (1979).
29. De Gennes P. G.: *J. Chem. Phys.* 55, 572 (1971).
30. Phuong-Nguyen H., Delmas G.: *Macromolecules* 12, 740 (1979).
31. Charlet G., Delmas G.: *Polymer* 22, 1181 (1981).
32. Bohossian T., Delmas G.: *J. Polym. Sci., Polym. Phys. Ed.* 30, 993 (1992).
33. Blackadder D. A., Le Poidevin G. J.: *Polymer* 19, 483 (1978).
34. Okabe M., Ukaji T.: *Ikutoku Kogyo Daigaku Kenkyu Hokoku, B B-12*, 167 (1988); *Chem. Abstr.* 109, 38663 (1988).
35. Ferracini E., Ferrero A., Malta V., Martelli S., Vogel W.: *Colloid Polym. Sci.* 269, 1241 (1991).
36. Geil P. H.: *Polymer Single Crystals*. Krieger Publishing Co., Huntington 1973.